

# A Novel Method for Detecting Genetic Biomarkers in Blood-based Liquid Biopsies Using Surface Plasmon Resonance Imaging and Magnetic Beads Shows Promise in Cancer Diagnosis and Monitoring

Noemi Bellassai<sup>1,2</sup>, Roberta D'Agata<sup>1,2</sup>, Elena Giordani<sup>3</sup>, Giovanna Ziccheddu<sup>3</sup>, Roberto Corradini<sup>4</sup>, Giuseppe Spoto<sup>1,2\*</sup>

<sup>1</sup> Department of Chemical Sciences, University of Catania, Viale Andrea Doria 6, 95122, Catania, Italy.

<sup>2</sup> INBB, Istituto Nazionale di Biostrutture e Biosistemi, Viale delle Medaglie d'Oro, 305, 00136 Roma, Italy.

<sup>3</sup> Oncogenomics and Epigenetics, IRCSS Regina Elena National Cancer Institute, Via Elio Chianesi, 53, 00144 Rome, Italy.

<sup>4</sup> Department of Chemistry, Life Sciences and Environmental Sustainability, University of Parma, Parco Area Delle Scienze, 17/A, 43124, Parma, Italy.

\*Email: [giuseppe.spoto@unict.it](mailto:giuseppe.spoto@unict.it)

**ABSTRACT:** Directly detecting biomarkers in liquid biopsy for diagnosis and personalized treatment plays a crucial role in managing cancer relapse and increasing survival rates. Typically, the standard analysis of circulating tumour DNA requires lengthy isolation, extraction, and amplification steps, leading to sample contamination, longer turnaround time and higher assay costs. Surface plasmon resonance is an emerging and promising technology for rapid and real-time dynamic biomarker monitoring in liquid biopsy. Here, we propose a new SPR imaging biosensing approach to detect tumour DNA circulating in the blood of colorectal cancer patients by exploiting the unique properties of superparamagnetic particles. Micrometer beads functionalized with a biotinylated oligonucleotide can directly capture DNA target sequences bearing single-nucleotide variations of KRAS oncogene in human blood plasma. Mutated and wild-type peptide nucleic acid probes immobilized on an SPR gold surface recognize complementary and non-complementary DNA targets by discriminating a single nucleotide mismatch. The new assay allows for detecting p.G13D mutated DNA in buffer and spiked human plasma at attomolar level (down to 300 copies mL<sup>-1</sup>) with minimal sample manipulation and in just a few microliters. The assay was validated using plasma samples from colorectal cancer patients and healthy donors, by discriminating mutated DNA circulating in patients and wild-type DNA found in healthy blood donors. This feature underscores the potential of the liquid biopsy assay as a valuable tool for the diagnosis and monitoring of cancer.

**KEYWORDS.** Superparamagnetic particles; surface plasmon resonance; circulating tumour DNA; peptide nucleic acids, KRAS.

## 1. Introduction

Liquid biopsy (LB) has become increasingly attractive for monitoring cancer biomarkers circulating in body fluids [1–4]. This approach provides easily repeatable tumour diagnostics over time [5,6], essential for clinical management [4], and reduces healthcare costs [3], making it potentially accessible even in low- and middle-income countries. Cancer biomarkers include circulating tumour DNA (ctDNA), circulating tumour cells (CTCs), and exosomes, but many other tumour components are shed into body fluids, providing tumour and non-tumour-derived information to capture cancer-associated analytes [7,8]. Next-generation sequencing (NGS) technologies, both targeted and whole-genome (WGS), are available to detect ctDNA [9]. Alternatively, digital polymerase chain reaction (dPCR) enables the detection of a limited number of species per run [10,11], and the isolation of ctDNA from the patient's plasma, its amplification and analysis in buffered solutions [12,13]. The complexity of pre-analytical procedures, potential analyte decomposition and sample contamination increase with workflow steps and analysis time. NGS and dPCR need mandatory pre-analytical sample processing, involve expensive and labour equipment and time-consuming protocols to detect circulating genomic alterations, which hamper ctDNA detection in point-of-care devices [14,15]. Compared to the above-discussed technologies, some biosensing platforms offer several advantages: limited pre-analytical processing, no amplification, fast turnaround time and limited cost per analysis. Surface plasmon resonance (SPR) technologies are reliable optical biosensors for real-time monitoring of the binding between biomolecules. The high sensitivity makes SPR the right choice for various applications [16–18]. Especially in LB, designing novel, robust and effective interfaces is pivotal to ensuring accurate and reliable SPR detection of different molecular interactions [19]. Also, functional surface architectures minimise non-specific adsorption while maintaining high analytical performances of the biosensing platform [20–23]. Moreover, combining metallic nanoparticles with SPR biosensing allowed ultra-sensitive detection in concentration ranges as low as attomolar, even in blood samples [24,25].

In recent years, magnetic beads have become increasingly attractive for their peculiar features, such as the high surface area to volume ratio that maximises the number of immobilised receptors and the straightforward and rapid separation of the modified beads. Also, using magnetic beads in bioassays allows for precise shaking and incubation temperature control [26–28].

Here, we present a new SPR imaging (SPRI)-based method using superparamagnetic beads for the diagnosis and monitoring of colorectal cancer (CRC) patients through LB. The new plasmonic platform detects single nucleotide variants (SNVs) identified in the Kirsten RAS (KRAS) gene, specifically in exon 2 at codons 12 and 13 of ctDNA from CRC patients [29,30]. Our new method

includes the functionalization of streptavidin-coated superparamagnetic beads (1  $\mu\text{m}$  in diameter) with a biotinylated oligonucleotide to catch and rapidly isolate cell-free DNA (cfDNA) from patients' blood plasma. We have integrated the cfDNA capturing capacity of functionalized beads with SPRI biosensing using peptide nucleic acid (PNA) probes to introduce selectivity for ctDNA sequences. This approach ensures outstanding performance in the detection of five single nucleotide variations (SNVs) in KRAS oncogene and wild-type DNA spiked into buffer and pooled human plasma at very low concentrations ( $1.0 \text{ pg } \mu\text{L}^{-1} \sim 0.5 \text{ aM}$  down to  $300 \text{ copies mL}^{-1}$ ). Finally, we utilized the SPRI assay to identify KRAS-mutated ctDNA in liquid biopsy samples (blood plasma) from CRC patients and healthy donors.

The new SPRI-based method provides a simpler and more effective analytical approach compared to standard methods like dPCR and NGS, as well as other recently proposed SPR-based methods for detecting ctDNA from liquid biopsies without PCR amplification [20,25,31–33]. This method emphasizes the capability for early-stage cancer progression analysis, especially when the concentration of oncogenic biomarkers may not be adequate for reliable detection [34].

## 2. Experimental section

The material and methods are summarized in the supplementary material.

## 3. Results and Discussion

### *3.1. Superparamagnetic beads-based SPRI detection of tumour gDNA spiked in buffer and human plasma*

We preliminarily evaluated the SPRI assay's performance by detecting KRAS mutated (p.G13D) gDNA spiked in PBS buffer or pooled human plasma.

### Workflow of the superparamagnetic beads-based plasmonic assay

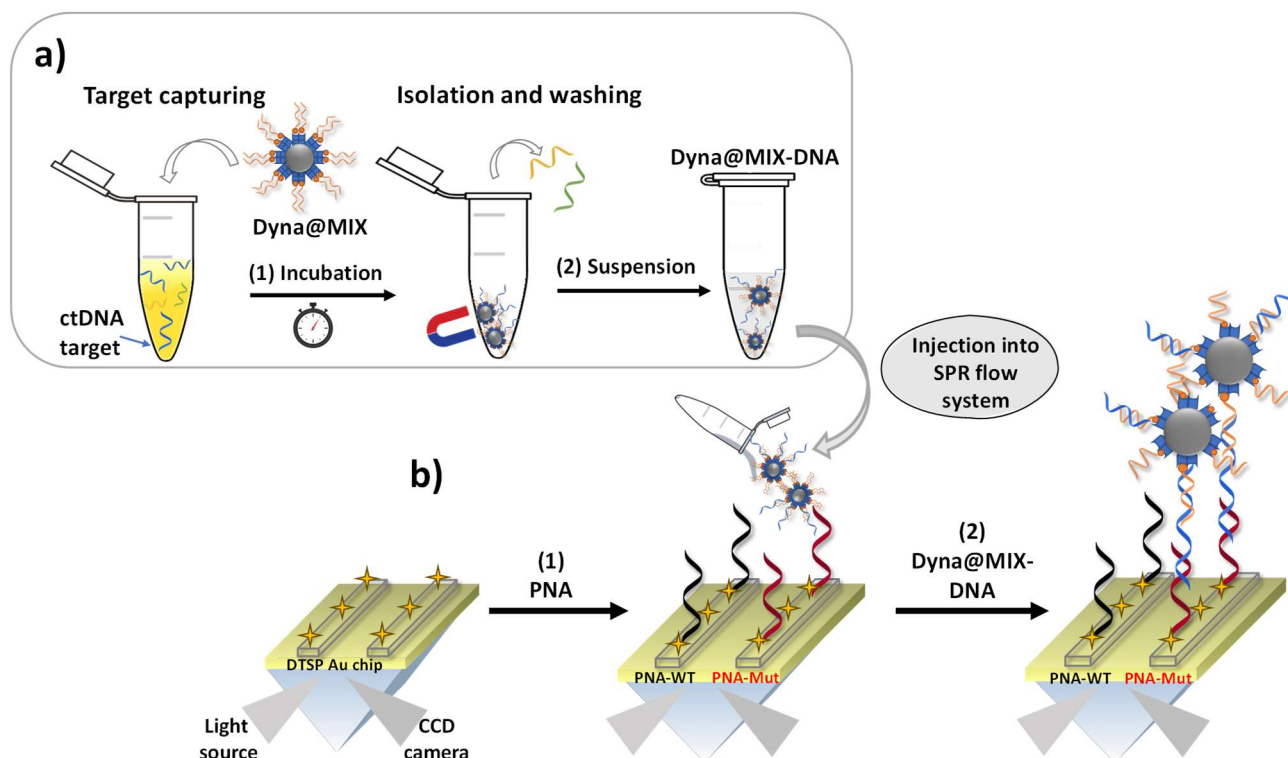


**Figure 1.** A pictorial description of the ultrasensitive detection of KRAS mutated ctDNA in human plasma samples using an SPR-based assay using superparamagnetic particles. To simplify the description, only specifically hybridized ctDNA is shown. (a) We captured ctDNA directly from a human plasma sample using superparamagnetic beads (Dyna@MIX) functionalized with an oligonucleotide sequence to obtain Dyna@MIX-DNA. (b) We covalently immobilized PNA-WT and PNA-Mut probes on a DTSP-modified gold SPRI sensor surface to discriminate KRAS mutated (ctDNA) and wild-type DNAs during the interaction with Dyna@MIX-DNA.

DTSP-modified gold surface exposes NHS ester moieties necessary for the amine coupling reaction with the N-terminus of PNA probes. This process ensures the covalent anchoring of PNA-WT and PNA-G13D probes ( $0.05 \mu\text{M}$  in PBS, 20 min, flow rate  $10 \mu\text{L min}^{-1}$ ) by injecting probe solutions into a microfluidic device bearing six parallel microchannels attached to the gold surface. The parameters and morphology of the microfluidic device are reported in the supplementary materials.

PNAs offer unique advantages in DNA hybridization by recognizing single-base mismatches with high selectivity at low and high temperatures or low target concentrations [20,24,35–37], if compared to homologous nucleic acid structures [38]. In addition, PNA has a remarkably long shelf life and remains intact even after 6 years of storage [26].

The use of microfluidic channels allowed us to achieve a spatially controlled immobilization density of PNA-WT and PNA-G13D probes on the SPRI gold surface, which affects the efficiency of PNA/DNA hybridization. The steric hindrance caused by the densely packed probes can negatively impact

the hybridization reaction [39]. Conversely, a low surface density reduces the number of PNA molecules available for DNA interaction [40]. Therefore, to successfully detect KRAS wild-type or p.G13D mutated DNAs, it is crucial to accurately monitor the probes' surface density by comparing the SPRI signals detected when PNA-WT and PNA-G13D probes are immobilized.

Figure 2 shows representative SPRI data for the parallel immobilization of PNA-WT and PNA-G13D probes.

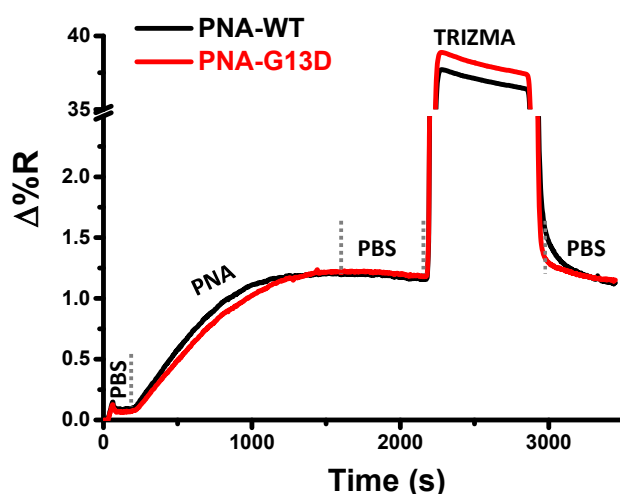


**Figure 2.**  $\Delta\%R$  over time detected for PNA-WT or PNA-G13D probes parallel immobilization ( $0.05 \mu\text{M}$ , 20 min) on DTSP functionalized gold surface. The y-axis displays a breakpoint related to Trizma's refractive index variation ( $\Delta\%R = 35$ ) to zoom in the kinetic profile of PNAs recorded during their immobilization.

After PNA immobilization (Fig. 1b step 1, Fig. 2), we favoured the desorption of unreacted molecules by flowing PBS onto the surface. Afterwards, an aqueous Trizma® hydrochloride solution ( $0.5 \text{ M}$  at  $\text{pH } 8.0$ ) was used to switch off the residual active NHS-end groups of the DTSP monolayer. To remove unbound molecules further and restore the refractive index level of the running buffer, we washed the PNA-WT and PNA-G13D modified gold surface with PBS for at least 10 minutes. A stable SPRI baseline recorded after the washing step indicates the final stabilization of the PNA-modified gold surface. As expected, a similar kinetic profile was recorded for both PNA probes since their sequences differ only from one single-base mismatch (Fig. 2).

SPRI signals (changes in per cent reflectivity  $\Delta\%R$  over time) allowed us to quantify the thickness of the surface layer and the probe surface coverage, as described by Shumaker-Parry et al.[41]. We achieved the probes' surface density corresponding to  $9 \cdot 10^{12} \text{ molecules cm}^{-2}$  by considering the refractive index and density of PNA molecules equal  $1.4$  and  $1.2 \text{ g cm}^{-3}$ , respectively. We calculated

a signal variability ranging from 6% to 7% (CV%) for PNA probes over ten parallel performed immobilizations. Probe immobilizations with  $CV\% \geq 15\%$  were discarded.

We fragmented KRAS wild-type gDNA isolated from HT-29 human cells, and KRAS p.G13D mutated gDNA isolated from LoVo cells ( $1.0 \text{ pg } \mu\text{L}^{-1}$  corresponding to  $285 \text{ copies mL}^{-1}$ , calculated by the following formula  $\text{DNA copies mL}^{-1} = \frac{(\text{DNA nanograms mL}^{-1} * 6.0221 * 10^{23})}{(\text{DNA base pairs} * \text{Molecular weight base pairs} * 10^9)}$ , with DNA base pairs (bp) in genome human aploid equal to  $3.2 \cdot 10^9$  and DNA bp molecular weight equal to  $660 \text{ g mol}^{-1}$ ) at the same concentration as ctDNA in the plasma of cancer patients. Superparamagnetic particles were grafted with the biotinylated oligoMIX sequence (Dyna@MIX) complementary to a shared region of KRAS exon carrying both the mutations under test (p.G12A, p.G12R, p.G12V, and p.G13D) and the corresponding wild-type sequence. Characterization of chemical properties by UV-vis spectra, AT-IR spectra, brightfield microscopy, particle size and zeta potential data of Dyna@MIX before and after the functionalization process have been reported in the supplementary information (Fig. S1-S3, Table S2). During the incubation (Fig. 1a step 1), oligoMIX hybridizes with a sequence portion not involved in the specific hybridization between the PNA probes and the KRAS mutated or wild-type target regions. OligoMIX modified magnetic particles (Dyna@MIX beads) with the captured gDNA sequence (Dyna@MIX-DNA) were magnetically isolated, washed three times and resuspended in  $20 \text{ } \mu\text{L}$  of PBS buffer before SPRI analysis (Fig. 1a step 2). We used an SPRI assay exploiting the hybridization of the Dyna@MIX-DNA captured WT gDNA or p.G13D mutated gDNA with the complementary PNA probe (PNA-WT or PNA-Mut) covalently bound to the SPRI sensor (Fig. 1b step 1). The final Dyna@MIX-DNA dispersion was introduced in two parallel channels of the SPRI microfluidic device for a few seconds and pushed by PBS buffer to reach the PNA-modified gold sensor surface. This approach allows comparing the plasmonic signals when the same DNA sample interacts with both complementary and non-complementary PNA probes (Fig. 1b step 2). The change in the SPRI detected signal caused by adsorbed Dyna@MIX-DNA was used to monitor the position of the beads in the fluidic system and to stop the pumping system when Dyna@MIX-DNA reached the SPRI gold sensor. As highlighted with arrows in Figures 3a and 3b, turning off the pumping system may slow down bead sedimentation and facilitate the binding of Dyna@MIX-DNA and PNA probes, resulting in a greater variation in the plasmonic signal related to the higher refractive index of the magnetic particles. After the reactivation of the pump, unbound and/or nonspecifically bound molecules were removed from the surface by generating slight changes in the SPRI signals. Such a procedure was adopted to minimize the volume of Dyna@MIX-DNA dispersion required for the analysis, thus avoiding diluting the

dispersion with the consequence of reduced assay sensitivity. The SPRI detection of Dyna@MIX-DNA beads, resulting from the incubation and isolation of  $1.0 \text{ pg } \mu\text{L}^{-1}$  KRAS wild-type gDNA through Dyna@MIX performed externally from plasmonic and microfluidic setup (off-line capture), highlighted a preferred interaction with the PNA-WT probe instead of the PNA-G13D probe (Fig. 3a). By contrast, a preferential interaction with PNA-G13D probe instead of PNA-WT was detected for the adsorption of Dyna@MIX-DNA beads resulting from the off-line capture of  $1.0 \text{ pg } \mu\text{L}^{-1}$  KRAS p.G13D gDNA (Fig. 3b).

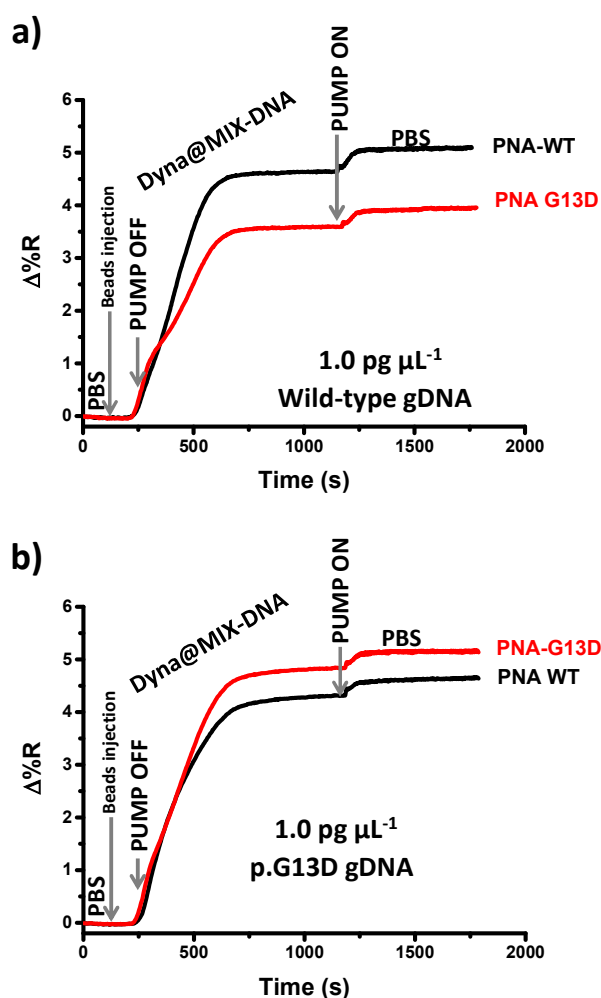


**Figure 3.** Representative time-dependent SPRI curves detected for the interaction between Dyna@MIX-DNA beads resulting from the capture of  $1.0 \text{ pg } \mu\text{L}^{-1}$  (a) KRAS wild-type and (b) KRAS p.G13D mutated gDNAs in PBS buffer and the surface-immobilized PNA-WT and PNA-G13D probes. As already described, the irregular shapes of curves shown in panels a and b were caused by the experimental procedure adopted to minimize the sample volume needed for the experiment that required the pumping system's stop when Dyna@MIX-DNA reached the sensor surface and its reactivation to replace the beads with PBS running buffer.

The simultaneously acquired SPR kinetic profiles shown in Figure 3 result from the parallel interaction between the relevant Dyna@MIX-DNA and the complementary and non-complementary



PNA probes, respectively. Combined with the design of PNA sequences, which differ by only a single mismatch (Table S1), such a feature can cause non-specific interactions between Dyna@MIX-DNA and the not complementary probe. To consider such an effect, we calculated the ratio of  $\Delta\%R$  values detected during the washing step at 1750 seconds, after the parallel interaction of Dyna@MIX-DNA with the complementary and non-complementary PNA probes (Fig. 3).

To simulate liquid biopsy samples from cancer patients, we spiked  $1.0 \text{ pg } \mu\text{L}^{-1}$  of KRAS p.G13D mutated gDNA in 1:5 diluted pooled human plasma from healthy donors and used the unspiked 1:5 diluted pooled human plasma from healthy donors as a proxy of KRAS wild-type liquid biopsy sample since circulating free DNA (cfDNA) is naturally present in human plasma. We adopted the dilution ratio 1:5 of pooled human plasma to further simplify the sample manipulation procedures and ensure effective discrimination signals. SPR experiments with a reduced dilution factor (1:2) of plasma samples did not provide satisfying results in DNA detection, by requiring at least detergents or other compounds to improve the assay (Fig. S4).

Figure 4 summarizes results from replicated independent analyses of the human plasma samples with only KRAS WT cfDNA, and plasma samples spiked with KRAS p.G13D mutated gDNA ( $1.0 \text{ pg } \mu\text{L}^{-1}$ ).

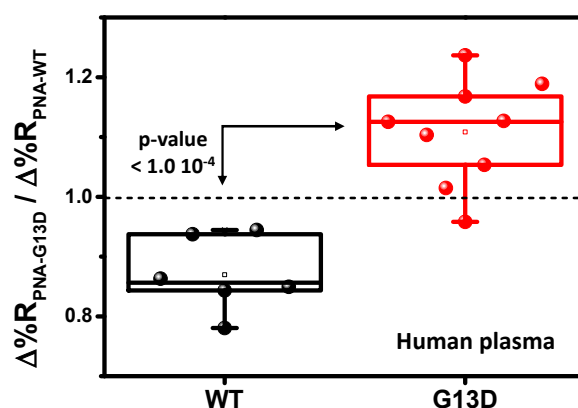


**Figure 4.**  $\Delta\%R_{\text{PNA-G13D}}/\Delta\%R_{\text{PNA-WT}}$  values obtained from replicated experiments aimed at detecting KRAS p.G13D mutated gDNAs spiked in pooled human plasma samples from healthy donors (final dilution 1:5) at  $1.0 \text{ pg } \mu\text{L}^{-1}$  final concentration and KRAS WT cfDNA in the unspiked pooled plasma from healthy donors. Ratios were obtained by considering  $\Delta\%R$  values after 1750 s of the hybridization step between Dyna@MIX-DNA and PNA probes complementary and not complementary to the target sequence. A dotted line highlights the values of the  $\Delta\%R_{\text{PNA-G13D}}/\Delta\%R_{\text{PNA-WT}}$  ratios below and beyond 1 obtained for each experiment.

The population mean value of  $\Delta\%R_{\text{PNA-G13D}}/\Delta\%R_{\text{PNA-WT}}$  ratios calculated after SPRI analysis of  $1.0 \text{ pg } \mu\text{L}^{-1}$  KRAS p.G13D mutated DNA samples (population mean confidence interval at the 95% level for the ratio  $\text{CI} = 1.11 \pm 0.09$ ,  $n=9$ ) was different from that of wild-type cfDNA samples ( $\Delta\%R_{\text{PNA-}}$

$G13D/\Delta\%R_{PNA-WT}$  95% CI =  $0.87 \pm 0.06$ ,  $n=6$ . Two-tailed t-test, level 95%,  $p$ -value  $<1.0 \cdot 10^{-4}$ ) (Table S3).

Based on what was reported for other assays using similar beads [28,42], the sensitivity enhancement for DNA detection can be ascribed to the synergic contribution of several factors, including the inherent magnetic properties of the beads, the off-line target capturing, the reduction of non-specific binding of interfering substances, and the clustering of Dyna@MIX-DNA triggered by the beads interaction with the PNA probe. The small and uniform size of the beads leads to a high surface area per mg of beads and a correspondingly high loading capacity ( $3\text{--}4 \cdot 10^5$  oligoMIX molecules/bead) available to drive the reaction  $\text{DNA} + \text{Dyna@MIX} \rightleftharpoons [\text{Dyna@MIX-DNA}]$  to the equilibrium towards binding and facilitate efficient capture of target DNA [42]. These features merged to a slow sedimentation rate during the beads' incubation with target DNA, contributing to a rapid magnetic separation and target isolation. Also, the glycidyl ether hydrophilic shell of the beads' surface allows the covalent immobilization of a streptavidin monolayer with a negligible protein leakage and, by concealing the iron oxide inside, it minimizes the non-specific adsorption of interfering biomolecules limiting the aggregation of beads in the biological environment [18].

The ultrahigh sensitivity we achieved using our plasmonic assay can also be attributed to mass and refractive index enhancement from clustered magnetic particle conjugates on the SPR chip. We hypothesised that Dyna@MIX-DNA specific hybridization with PNA probe could trigger the accumulation of further beads, as predicted for single magnetic domain-induced superparamagnetic particle aggregation [43–45]. A similar process has already been demonstrated for nucleic acid sequence-induced aggregation of metallic nanoparticles [46].

We calculated the average surface density of Dyna@MIX-DNA bearing KRAS p.G13D mutated DNA and adsorbed on specific (PNA-G13D) and control (PNA-WT) probes, using the model by Shumaker-Parry et al.[41] (density and refractive index of magnetic beads  $1.7 \text{ g cm}^{-3}$  and  $1.6$  [47]). The adsorbate surface coverage corresponds to  $965 \text{ pg mm}^{-2}$  for PNA-G13D and  $854 \text{ pg mm}^{-2}$  for PNA-WT in human plasma samples, while lower surface coverage values in PBS during the interaction with the specific and control probes ( $854 \text{ pg mm}^{-2}$  and  $629 \text{ pg mm}^{-2}$ , respectively) have been obtained. The slight increase (13%) in the absorbate mass from PBS buffer to human plasma samples, indicating a limited contribution of non-specifically adsorbed species onto the beads during ctDNA capture in pooled plasma, did not prevent the discrimination between human plasma samples carrying KRAS p.G13D mutated or WT DNA, as shown in Figure 4.

To verify the functioning of the plasmonic assay in SNV recognition, we also carried out an SPR experiment with  $1.0 \text{ pg } \mu\text{L}^{-1}$  of wild-type gDNA isolated from HT-29 cells and spiked in 1:5 diluted

pooled human plasma from healthy donors. When comparing the analysis of both unspiked plasma samples and those spiked with KRAS p.G13D mutated gDNA, we observed comparable SPR signal discrimination. This confirmed the intended working principle of our assay, along with Dyna@MIX, in both tests (Fig. S5).

### 3.2. Superparamagnetic beads-based SPRI detection of tumour DNA in liquid biopsy samples

Therefore, we moved to detect KRAS-mutated DNA circulating in the blood of metastatic patients by adopting the already described procedures. Samples from CRC patients (pt#40 - KRAS p.G12A mutated; pt#50 - KRAS p.G12R mutated; pt#33 - KRAS p.G12V mutated; pt#34 - KRAS p.G13D mutated) and healthy donor (sample#16 - KRAS wild-type) were preliminarily validated by NGS and dPCR (Table S4) (Allegretti et al., 2020; D'Agata et al., 2020). Representative SPRI curves for detecting KRAS p.G13D mutated ctDNA (sample pt#34) and wild-type cfDNA from a healthy donor (#16) were reported in the supplementary information (Fig. S6).

Figure 5 shows  $\Delta\%R_{\text{PNA-Mut}}/\Delta\%R_{\text{PNA-WT}}$  ratios obtained from replicated independent analyses of liquid biopsies from CRC patients (pt#40, pt#50, pt#33, and pt#34 samples) and a healthy donor (sample#16). Each experiment was performed by analyzing a sample from a healthy donor that acted as the control for the assay in parallel with each CRC patient sample.

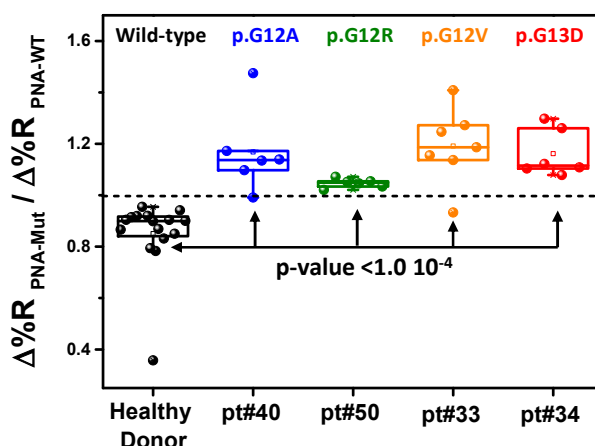


**Figure 5.** Box plots of  $\Delta\%R_{\text{PNA-Mut}}/\Delta\%R_{\text{PNA-WT}}$  ratios calculated after the hybridization of Dyna@MIX-DNA from CRC patients and healthy donor plasma samples with PNA probes for p.G12A, p.G12R, p.G12V, p.G13D KRAS mutated and WT DNAs. Plasma samples (pt#40, pt#50, pt#33, and pt#34) from CRC patients with KRAS mutated ctDNAs provided values of the ratio greater than 1 in all cases (25) with two exceptions (p.G12A and p.G12V), whereas plasma samples from healthy donors (WT cfDNA) provided values smaller than 1 for all cases.

$\Delta\%R_{\text{PNA-Mut}}/\Delta\%R_{\text{PNA-WT}}$  ratios obtained for pt#40, pt#50, pt#33, and pt#34 plasma samples were significantly and extremely significantly statistically different than those for plasma from a healthy

donor. Population mean confidence intervals at the 95% level of  $\Delta\%R_{\text{PNA-Mut}}/\Delta\%R_{\text{PNA-WT}}$  ratios for the analyzed liquid biopsies are reported in Table S5, together with samples ID, the number of replicates and p-values (CRC patient and healthy donor mean comparison. Two-tailed t-test).

These results confirm that the designed assay offers a novel platform for the facile detection of mutated tumour DNA in plasma samples. The new assay can detect ctDNA and cfDNA in plasma samples after minimal and rapid pre-analytical processing with no target PCR amplifications by adopting a three steps workflow: off-line target catching in plasma by Dyna@MIX, PNA probes immobilization, and parallel interaction of Dyna@MIX-DNA and complementary and non-complementary PNA probes. The total turnaround time, including DNA fragmentation and denaturation (10 min), DNA capture by Dyna@MIX (60 min), and PNA immobilization (50 min) - these procedures are performed simultaneously-, and the hybridization of Dyna@MIX-DNA with PNA probes (30 min), is only 100 minutes. The target capture by Dyna@MIX in human plasma minimizes the non-specific adsorption of interfering species from the biofluids, which can alter the detected SPR responses. In addition, the Dyna@MIX capture of ctDNA and/or cfDNA requires a small dilution (1:5) of the sample with volumes as low as 20  $\mu\text{L}$  of human plasma.

The new SPRI-based method introduced here brings significant innovations compared to other SPRI biosensing approaches for detecting ctDNA in liquid biopsy. This new method has the potential to greatly impact future cancer diagnostics based on liquid biopsy due to its simple analytical protocol and the reduced blood sample volume required for analysis [20,25]. The off-line target capture by Dyna@MIX and straightforward beads isolation by simply using an external magnet enabled us to simplify the entire workflow in three steps. The external magnetic handling enables easy washing, separation, and concentration of target sequences directly into biofluids, by removing other biological compounds which could interfere with the plasmonic assay. After the off-line capture, the resuspension of Dyna@MIX-DNA in PBS buffer eliminates the need to create an antifouling layer on the biosensor's active surface, typically involving 5 workflow steps. It also eliminates the need to treat the sensor surface with dithiothreitol to remove nonspecifically adsorbed protein or to use other blocking agents after plasma adsorption, a process that usually involves 4 workflow steps. A similar approach cannot be implemented with the metallic nanoparticles often used to enhance SPR responses. The size and metallic properties difference between superparamagnetic particles (1  $\mu\text{m}$ ) and colloidal nanoparticles (at nanometer scale) enables the direct capture of circulating biomarkers from biofluids with easy separation of the beads after the target enrichment. Furthermore, the assay time has been decreased to less than 2 hours, in comparison to the 2.5 hours required for other SPRI-based methods. The sample volume necessary for reliable analysis has been reduced by half, from 40

to 20  $\mu\text{L}$ , with a minimal dilution factor of 1:5, as opposed to 1:10. This reduction limits protein denaturation at high temperatures, by addressing issues present in previous plasmonic assays where high dilution factors and blocking additives have been used.

#### 4. Conclusion

The critical achievement described here is the implementation of the SPRI assay with the use of superparamagnetic beads able to catch complementary DNA sequences directly in blood-plasma and enhance the detection of mutated KRAS gene. After the capture of DNA sequences by Dyna@MIX, the hybridization between Dyna@MIX-DNA bearing the caught target and complementary and non-complementary PNA probes immobilized on the plasmonic biosensor enables the detection KRAS oncogene by recording SPRI responses. The synergic role of beads in enhancing the plasmonic signals and the inherent properties of PNA probes allowed us to achieve the detection of less than 300 copies  $\text{mL}^{-1}$  of KRAS p.G13D mutated DNA and discrimination between KRAS mutated and wild-type samples in human plasma by employing a minimum sample volume (20  $\mu\text{L}$ ) per single analysis. The assay also confirmed the correct identification of KRAS mutated ctDNA in plasma from CRC patients and wild-type cfDNA in plasma from healthy donors by demonstrating the assay's analytical and clinical validity in testing liquid biopsies from CRC patients.

With this approach, several cumbersome steps in analyzing liquid biopsy samples from cancer patients (e.g., temperature cycling, sample carryover, and sample transfer to different pieces of equipment, such as different types of centrifuges and purification devices) are no longer required. In conclusion, the new SPRI biosensing strategy, based on superparamagnetic particles, offers rapid, PCR amplification-free, and straightforward detection of tumour-derived genetic materials circulating in human plasma. This breakthrough in cancer clinical diagnosis and personalized medicine, based on liquid biopsy, can potentially make a significant impact.

#### CRedit authorship contribution statement

**Noemi Bellassai:** Conceptualization, Methodology, Writing – original draft, Investigation, Formal analysis, Data curation. **Roberta D’Agata:** Writing – review & editing. **Elena Giordani:** Formal analysis, Data curation, Writing – review & editing. **Giovanna Ziccheddu:** Formal analysis, Data curation, Writing – review & editing. **Roberto Corradini:** Formal analysis, Data curation, Writing – review & editing. **Giuseppe Spoto:** Writing – review & editing, Supervision, Resources, Methodology, Funding acquisition, Formal analysis, Conceptualization.

## Declaration of Competing Interest

The authors declare that they have no known competing financial interests or personal relationships that could have appeared to influence the work reported in this paper.

## Acknowledgements

We acknowledge support from the European Innovation Council (EIC) under Horizon Europe program, grant agreement No 101046217 project VERSILIB. N.B. thanks research and innovation programme 2014-2020 "PON REACT-EU project".

## Appendix A. Supporting information

Supplementary data associated with this article can be found in the online version at ...

## References

- [1] C. Alix-Panabieres, Perspective: The future of liquid biopsy, *Nature* 579 (2020) S9.
- [2] T. Assi, R. Khoury, R. Ibrahim, M. Baz, T. Ibrahim, A. LE Cesne, Overview of the role of liquid biopsy in cancer management, *Transl Oncol* 34 (2023) 101702. <https://doi.org/https://doi.org/10.1016/j.tranon.2023.101702>.
- [3] G. De Rubis, S. Rajeev Krishnan, M. Bebawy, Liquid Biopsies in Cancer Diagnosis, Monitoring, and Prognosis., *Trends Pharmacol Sci* 40 (2019) 172–186. <https://doi.org/10.1016/j.tips.2019.01.006>.
- [4] J.D. Merker, G.R. Oxnard, C. Compton, M. Diehn, P. Hurley, A.J. Lazar, N. Lindeman, C.M. Lockwood, A.J. Rai, R.L. Schilsky, A.M. Tsimberidou, P. Vasalos, B.L. Billman, T.K. Oliver, S.S. Bruinooge, D.F. Hayes, N.C. Turner, Circulating Tumor DNA Analysis in Patients With Cancer: American Society of Clinical Oncology and College of American Pathologists Joint Review, *Arch Pathol Lab Med* 142 (2018) 1242–1253. <https://doi.org/10.5858/arpa.2018-0901-SA>.
- [5] J.J. Adashek, F. Janku, R. Kurzrock, Signed in Blood: Circulating Tumor DNA in Cancer Diagnosis, Treatment and Screening., *Cancers (Basel)* 13 (2021). <https://doi.org/10.3390/cancers13143600>.
- [6] B. Arneth, Update on the types and usage of liquid biopsies in the clinical setting: a systematic review., *BMC Cancer* 18 (2018) 527. <https://doi.org/10.1186/s12885-018-4433-3>.
- [7] J.M. Cameron, A. Sala, G. Antoniou, P.M. Brennan, H.J. Butler, J.J.A. Conn, S. Connal, T. Curran, M.G. Hegarty, R.G. McHardy, D. Orringer, D.S. Palmer, B.R. Smith, M.J. Baker, A spectroscopic liquid biopsy for the earlier detection of multiple cancer types., *Br J Cancer* 129 (2023) 1658–1666. <https://doi.org/10.1038/s41416-023-02423-7>.
- [8] G. Putcha, T.-Y. Liu, E. Ariazi, M. Bertin, A. Drake, M. Dzamba, G. Hogan, S. Kothen-Hill, J. Liao, K. Li, S. Mahajan, K. Palaniappan, P. Sansanwal, J. St John, P. Ulz, N. Wan, H. Warsinske, D. Weinberg, R. Yang, J. Lin, Blood-based detection of early-stage colorectal cancer using multiomics and machine learning., *Journal of Clinical Oncology* 38 (2020) 66. [https://doi.org/10.1200/JCO.2020.38.4\\_suppl.66](https://doi.org/10.1200/JCO.2020.38.4_suppl.66).
- [9] H. Li, C. Jing, J. Wu, J. Ni, H. Sha, X. Xu, Y. Du, R. Lou, S. Dong, J. Feng, Circulating tumor DNA detection: A potential tool for colorectal cancer management., *Oncol Lett* 17 (2019) 1409–1416. <https://doi.org/10.3892/ol.2018.9794>.

- [10] C.M. Hindson, J.R. Chevillet, H.A. Briggs, E.N. Gallichotte, I.K. Ruf, B.J. Hindson, R.L. Vessella, M. Tewari, Absolute quantification by droplet digital PCR versus analog real-time PCR, *Nat Methods* 10 (2013) 1003–1005. <https://doi.org/10.1038/nmeth.2633>.
- [11] B. Vogelstein, K.W. Kinzler, Digital PCR, *Proceedings of the National Academy of Sciences* 96 (1999) 9236–9241. <https://doi.org/10.1073/pnas.96.16.9236>.
- [12] I.W. Deveson, B. Gong, K. Lai, J.S. LoCoco, T.A. Richmond, J. Schageman, Z. Zhang, N. Novorodovskaya, J.C. Willey, W. Jones, R. Kusko, G. Chen, B.S. Madala, J. Blackburn, I. Stevanovski, A. Bhandari, D. Close, J. Conroy, M. Hubank, N. Marella, P.A. Mieczkowski, F. Qiu, R. Sebra, D. Stetson, L. Sun, P. Szankasi, H. Tan, L. Tang, H. Arib, H. Best, B. Burgher, P.R. Bushel, F. Casey, S. Cawley, C.-J. Chang, J. Choi, J. Dinis, D. Duncan, A.K. Eterovic, L. Feng, A. Ghosal, K. Giorda, S. Glenn, S. Happe, N. Haseley, K. Horvath, L.-Y. Hung, M. Jarosz, G. Kushwaha, D. Li, Q.-Z. Li, Z. Li, L.-C. Liu, Z. Liu, C. Ma, C.E. Mason, D.B. Megherbi, T. Morrison, C. Pabón-Peña, M. Pirooznia, P.Z. Proszek, A. Raymond, P. Rindler, R. Ringler, A. Scherer, R. Shaknovich, T. Shi, M. Smith, P. Song, M. Strahl, V.J. Thodima, N. Tom, S. Verma, J. Wang, L. Wu, W. Xiao, C. Xu, M. Yang, G. Zhang, S. Zhang, Y. Zhang, L. Shi, W. Tong, D.J. Johann, T.R. Mercer, J. Xu, S.O.S.W. Group, Evaluating the analytical validity of circulating tumor DNA sequencing assays for precision oncology, *Nat Biotechnol* 39 (2021) 1115–1128. <https://doi.org/10.1038/s41587-021-00857-z>.
- [13] F. Pittella-Silva, Y.M. Chin, H.T. Chan, S. Nagayama, E. Miyauchi, S.-K. Low, Y. Nakamura, Plasma or Serum: Which Is Preferable for Mutation Detection in Liquid Biopsy?, *Clin Chem* 66 (2020) 946–957. <https://doi.org/10.1093/clinchem/hvaa103>.
- [14] Y. Wang, S.L. Kong, X. Di Su, A centrifugation-assisted visual detection of SNP in circulating tumor DNA using gold nanoparticles coupled with isothermal amplification, *RSC Adv* 10 (2020) 1476–1483. <https://doi.org/10.1039/C9RA09029K>.
- [15] Y. Zhang, H. Noji, Digital Bioassays: Theory, Applications, and Perspectives, *Anal Chem* 89 (2017) 92–101. <https://doi.org/10.1021/acs.analchem.6b04290>.
- [16] A. Azzouz, L. Hejji, K.-H. Kim, D. Kukkar, B. Souhail, N. Bhardwaj, R.J.C. Brown, W. Zhang, Advances in surface plasmon resonance–based biosensor technologies for cancer biomarker detection, *Biosens Bioelectron* 197 (2022) 113767. <https://doi.org/https://doi.org/10.1016/j.bios.2021.113767>.
- [17] N. Bellassai, R. D’Agata, G. Spoto, Plasmonic aptasensor with antifouling dual-functional surface layer for lysozyme detection in food., *Anal Chim Acta* 1283 (2023) 341979. <https://doi.org/10.1016/j.aca.2023.341979>.
- [18] A. Kausaite-Minkstiniene, A. Popov, A. Ramanaviciene, Ultra-sensitive SPR immunosensors: A comprehensive review of labeling and interface modification using nanostructures, *TrAC - Trends in Analytical Chemistry* 170 (2024) 117468. <https://doi.org/10.1016/j.trac.2023.117468>.
- [19] R. D’Agata, N. Bellassai, G. Spoto, Exploiting the design of surface plasmon resonance interfaces for better diagnostics: A perspective review, *Talanta* 266 (2024) 125033. <https://doi.org/https://doi.org/10.1016/j.talanta.2023.125033>.
- [20] N. Bellassai, R. D’Agata, A. Marti, A. Rozzi, S. Volpi, M. Allegretti, R. Corradini, P. Giacomini, J. Huskens, G. Spoto, Detection of Tumor DNA in Human Plasma with a Functional PLL-Based Surface Layer and Plasmonic Biosensing, *ACS Sens* 6 (2021) 2307–2319. <https://doi.org/10.1021/acssensors.1c00360>.

- [21] D. Chen, Y. Wu, S. Hoque, R.D. Tilley, J.J. Gooding, Rapid and ultrasensitive electrochemical detection of circulating tumor DNA by hybridization on the network of gold-coated magnetic nanoparticles, *Chem. Sci.* 12 (2021) 5196–5201. <https://doi.org/10.1039/D1SC01044A>.
- [22] J. Das, I. Ivanov, L. Montermini, J. Rak, E.H. Sargent, S.O. Kelley, An electrochemical clamp assay for direct, rapid analysis of circulating nucleic acids in serum., *Nat Chem* 7 (2015) 569–575. <https://doi.org/10.1038/nchem.2270>.
- [23] N. Bellassai, R. D'Agata, V. Jungbluth, G. Spoto, Surface Plasmon Resonance for Biomarker Detection: Advances in Non-invasive Cancer Diagnosis, *Front Chem* 7 (2019) 1–16. <https://doi.org/10.3389/fchem.2019.00570>.
- [24] M. Calcagno, R. D'Agata, G. Breveglieri, M. Borgatti, N. Bellassai, R. Gambari, G. Spoto, Nanoparticle-Enhanced Surface Plasmon Resonance Imaging Enables the Ultrasensitive Detection of Non-Amplified Cell-Free Fetal DNA for Non-Invasive Prenatal Testing, *Anal Chem* 94 (2022) 1118–1125. <https://doi.org/10.1021/acs.analchem.1c04196>.
- [25] R. D'Agata, N. Bellassai, M. Allegretti, A. Rozzi, S. Korom, A. Manicardi, E. Melucci, E. Pescarmona, R. Corradini, P. Giacomini, G. Spoto, Direct plasmonic detection of circulating RAS mutated DNA in colorectal cancer patients, *Biosens Bioelectron* 170 (2020) 112648. <https://doi.org/https://doi.org/10.1016/j.bios.2020.112648>.
- [26] S. Fortunati, C. Giliberti, M. Giannetto, A. Bertucci, S. Capodaglio, E. Ricciardi, P. Giacomini, V. Bianchi, A. Boni, I. De Munari, R. Corradini, M. Careri, A highly sensitive electrochemical magnetogenosensing assay for the specific detection of a single nucleotide variation in the KRAS oncogene in human plasma, *Biosens Bioelectron X* 15 (2023) 100404. <https://doi.org/https://doi.org/10.1016/j.biosx.2023.100404>.
- [27] M. Mattarozzi, L. Toma, A. Bertucci, M. Giannetto, M. Careri, Aptamer-based assays: strategies in the use of aptamers conjugated to magnetic micro- and nanobeads as recognition elements in food control, *Anal Bioanal Chem* 414 (2022) 63–74. <https://doi.org/10.1007/s00216-021-03501-6>.
- [28] Y. Xianyu, Q. Wang, Y. Chen, Magnetic particles-enabled biosensors for point-of-care testing, *TrAC Trends in Analytical Chemistry* 106 (2018) 213–224. <https://doi.org/https://doi.org/10.1016/j.trac.2018.07.010>.
- [29] J. Timar, K. Kashofer, Molecular epidemiology and diagnostics of KRAS mutations in human cancer, *Cancer and Metastasis Reviews* 39 (2020) 1029–1038. <https://doi.org/10.1007/s10555-020-09915-5>.
- [30] A. Mullard, Cracking KRAS, *Nat Rev Drug Discov* 18 (2019) 887–891. <https://doi.org/10.1038/d41573-019-00195-5>.
- [31] Z. Chen, C. Meng, X. Wang, J. Chen, J. Deng, T. Fan, L. Wang, H. Lin, H. Huang, S. Li, S. Sun, J. Qu, D. Fan, X. Zhang, Y. Liu, Y. Shao, H. Zhang, Ultrasensitive DNA Origami Plasmon Sensor for Accurate Detection in Circulating Tumor DNAs, *Laser Photon Rev* 2400035 (2024) 1–12. <https://doi.org/10.1002/lpor.202400035>.
- [32] W. Ning, C. Zhang, Z. Tian, M. Wu, Z. Luo, S. Hu, H. Pan, Y. Li,  $\Omega$ -shaped fiber optic LSPR biosensor based on mismatched hybridization chain reaction and gold nanoparticles for detection of circulating cell-free DNA, *Biosens Bioelectron* 228 (2023) 115175. <https://doi.org/10.1016/j.bios.2023.115175>.
- [33] A. Tadimety, Y. Zhang, K.M. Kready, T.J. Palinski, G.J. Tsongalis, J.X.J. Zhang, Design of peptide nucleic acid probes on plasmonic gold nanorods for detection of circulating tumor DNA point mutations, *Biosens Bioelectron* 130 (2019) 236–244. <https://doi.org/10.1016/j.bios.2019.01.045>.



- [34] E.A. Klein, D. Richards, A. Cohn, M. Tummala, R. Lapham, D. Cosgrove, G. Chung, J. Clement, J. Gao, N. Hunkapiller, A. Jamshidi, K.N. Kurtzman, M. V Seiden, C. Swanton, M.C. Liu, Clinical validation of a targeted methylation-based multi-cancer early detection test using an independent validation set., *Ann Oncol* 32 (2021) 1167–1177. <https://doi.org/10.1016/j.annonc.2021.05.806>.
- [35] G. (Giuseppe) Spoto, Roberto. Corradini, *Detection of non-amplified genomic DNA*, Springer, 2012.
- [36] C.S. Swenson, H.H. Lackey, E.J. Reece, J.M. Harris, J.M. Heemstra, E.M. Peterson, Evaluating the effect of ionic strength on PNA:DNA duplex formation kinetics, *RSC Chem Biol* 2 (2021) 1249–1256. <https://doi.org/10.1039/D1CB00025J>.
- [37] S. Volpi, A. Rozzi, N. Rivi, M. Neri, W. Knoll, R. Corradini, Submonomeric Strategy with Minimal Protection for the Synthesis of C(2)-Modified Peptide Nucleic Acids, *Org Lett* 23 (2021) 902–907. <https://doi.org/10.1021/acs.orglett.0c04116>.
- [38] N. Bellassai, R. D'Agata, G. Spoto, Novel nucleic acid origami structures and conventional molecular beacon-based platforms: a comparison in biosensing applications, *Anal Bioanal Chem* 413 (2021) 6063–6077. <https://doi.org/10.1007/s00216-021-03309-4>.
- [39] F. Xu, A.M. Pellino, W. Knoll, Electrostatic repulsion and steric hindrance effects of surface probe density on deoxyribonucleic acid (DNA)/peptide nucleic acid (PNA) hybridization, *Thin Solid Films* 516 (2008) 8634–8639. <https://doi.org/10.1016/j.tsf.2008.06.067>.
- [40] R. D'Agata, M.C. Giuffrida, G. Spoto, Peptide Nucleic Acid-Based Biosensors for Cancer Diagnosis, *Molecules* 22 (2017) 1–15. <https://doi.org/10.3390/molecules22111951>.
- [41] J.S. Shumaker-Parry, C.T. Campbell, Quantitative Methods for Spatially Resolved Adsorption/Desorption Measurements in Real Time by Surface Plasmon Resonance Microscopy, *Anal Chem* 76 (2004) 907–917. <https://doi.org/10.1021/ac034962a>.
- [42] S. Krishnan, V. Mani, D. Wasalathanthri, C. V Kumar, J.F. Rusling, Attomolar Detection of a Cancer Biomarker Protein in Serum by Surface Plasmon Resonance Using Superparamagnetic Particle Labels, *Angewandte Chemie International Edition* 50 (2011) 1175–1178. <https://doi.org/https://doi.org/10.1002/anie.201005607>.
- [43] G. Fonnum, C. Johansson, A. Molteberg, S. Mørup, E. Aksnes, Characterisation of Dynabeads® by magnetization measurements and Mössbauer spectroscopy, *J Magn Magn Mater* 293 (2005) 41–47. <https://doi.org/https://doi.org/10.1016/j.jmmm.2005.01.041>.
- [44] B. Issa, I.M. Obaidat, B.A. Albiss, Y. Haik, Magnetic nanoparticles: surface effects and properties related to biomedicine applications., *Int J Mol Sci* 14 (2013) 21266–21305. <https://doi.org/10.3390/ijms141121266>.
- [45] H. Kachkachi, D.A. Garanin, Magnetic Nanoparticles as Many-Spin Systems BT - Surface Effects in Magnetic Nanoparticles, in: D. Fiorani (Ed.), Springer US, Boston, MA, 2005: pp. 75–104. [https://doi.org/10.1007/0-387-26018-8\\_3](https://doi.org/10.1007/0-387-26018-8_3).
- [46] R. D'Agata, P. Palladino, G. Spoto, Streptavidin-coated gold nanoparticles: critical role of oligonucleotides on stability and fractal aggregation, *Beilstein Journal of Nanotechnology* 8 (2017) 1–11. <https://doi.org/10.3762/bjnano.8.1>.
- [47] L.E. Helseth, H.Z. Wen, P. Heinig, Th.M. Fischer, Magnetic Beads as Interfacial Nanoprobes, *Langmuir* 20 (2004) 6556–6559. <https://doi.org/10.1021/la049802o>.



## Graphical abstract

